The QCD chiral phase transition for different numbers of quark flavours

Francesca Cuteri,[a] Owe Philipsen[a,b,*] and Alessandro Sciarra[a,c]

[a] *ITP, Goethe Universität Frankfurt,*
Max-von-Laue-Str. 1, 60438 Frankfurt, Germany

[b] *John von Neumann Institute for Computing (NIC)*
at GSI, Planckstr. 1, 64291 Darmstadt, Germany

[c] *Frankfurt Institute for Advanced Studies (FIAS)-Goethe University,*
Ruth-Moufang-Str. 1, 60438 Frankfurt am Main, Germany
E-mail: cuteri@itp.uni-frankfurt.de, philipsen@itp.uni-frankfurt.de,
sciarra@itp.uni-frankfurt.de

We present results from a comprehensive study of the location of the chiral critical surface, which separates regions of first-order chiral transitions from analytic crossovers, in the bare parameter space of lattice QCD with unimproved staggered fermions. We study the theories with $N_{\mathrm{f}} \in [2, 8]$ and trace the chiral critical surface along diminishing lattice spacing, with $N_\tau = \{4, 6, 8\}$. This allows for an extrapolation to the lattice chiral limit, where the surface has to terminate in a tricritical line, employing known tricritical scaling relations. Knowing the phase structure in the lattice bare parameter space allows to draw conclusions for the approach to the continuum and chiral limits taken in the appropriate order. Our data provide evidence for the continuum chiral limit to feature a second-order transition for all $N_{\mathrm{f}} \in [2, 7]$. We perform an analogous scaling analysis with already published data from $N_{\mathrm{f}} = 3$ $O(a)$-improved Wilson fermions, which is also consistent with a second-order transition in the continuum. A modified Columbia plot reflecting those results is suggested.

The 38th International Symposium on Lattice Field Theory, LATTICE2021 26th-30th July, 2021
Zoom/Gather@Massachusetts Institute of Technology

---

*Speaker

(a) First-order scenario for $N_f = 2$, $m_{u,d} = 0$.

(b) Second-order scenario for $N_f = 2$, $m_{u,d} = 0$.
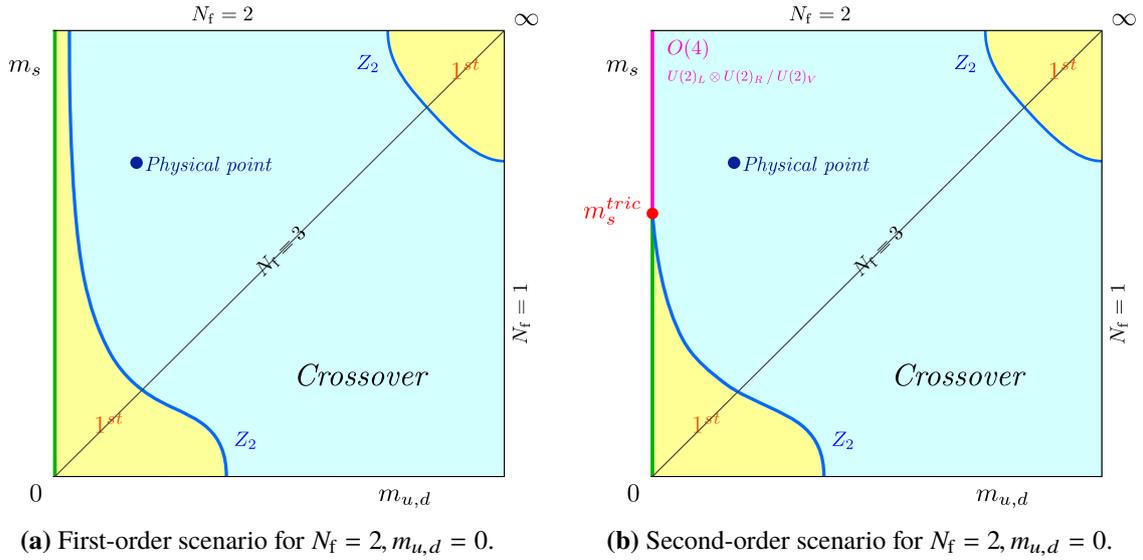
Figure 1: Possible scenarios for the order of the thermal QCD transition as a function of the quark masses.

1. Introduction

The nature of the QCD chiral phase transition in the limit of massless quarks has been a longstanding, open problem. Its unambiguous, non-perturbative resolution is important, because the light quarks in nature are close to the chiral limit. This raises the question whether traces of the chiral phase transition might be detectable experimentally. Unfortunately, direct lattice simulations of the chiral limit are not feasible due to the singular nature of the fermion determinant, so that extrapolations are inevitable, introducing systematic errors.

The nature of the thermal QCD transition with $N_f = 2 + 1$ flavours is usually displayed as a function of the quark masses in a Columbia plot [1], as in figure 1. The two possibilities correspond to the predictions of the renormalisation group flow in 3D sigma models, augmented by a 't Hooft term for the axial anomaly, using the epsilon expansion [2]: for $N_f \geq 3$ the chiral phase transition in the massless limit is predicted to be of first order, whereas for $N_f = 2$ it depends on whether the axial anomaly is effectively restored at the critical temperature (first order), or remains broken (second order). Numerous numerical lattice investigations have been devoted to determine the location of the second-order boundaries to distinguish between these scenarios. One generally observes widely differing values for the pseudo-scalar mass evaluated on the critical boundary at different points and between different actions. Unimproved staggered and Wilson actions as well as $O(a)$-improved Wilson actions on coarse lattices see a first-order region both for $N_f \in \{2, 3\}$, but it is found to shrink drastically as the lattice is made finer [3–12]. On the other hand, improved staggered actions do not see a first-order region at all down to $m_{PS} \approx 50$ MeV [13]. For a detailed review, see [14]. The question is whether there are actual contradictions between different discretisations, or whether they all converge towards one answer, and whether the correct answer has any first-order region in the continuum limit. Here we discuss a novel way to analyse the cutoff effects associated with the observed first-order region, which suggests a unified description of all available lattice results.
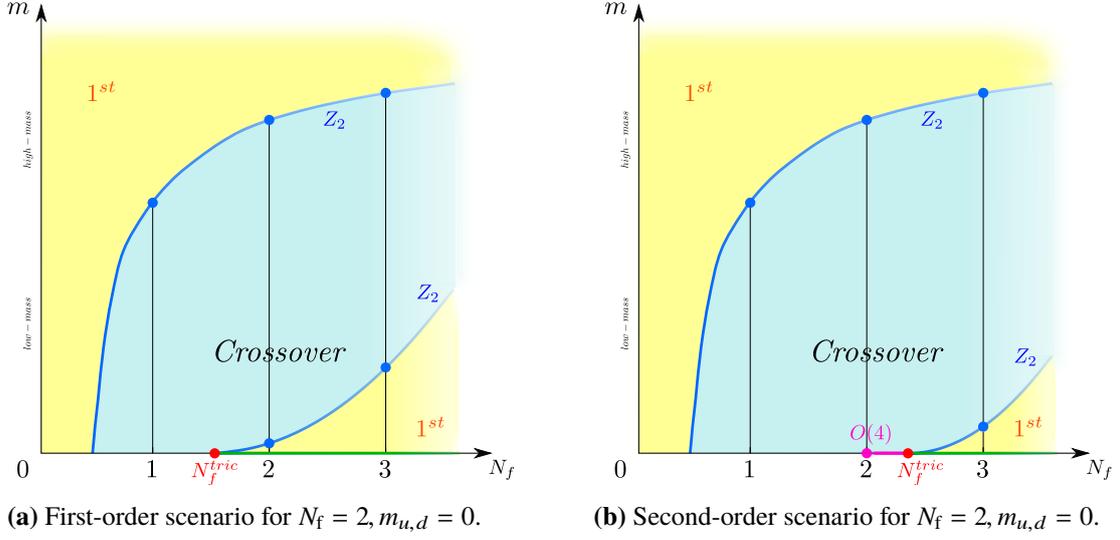
(a) First-order scenario for $N_f = 2, m_{u,d} = 0$.   **(b)** Second-order scenario for $N_f = 2, m_{u,d} = 0$.

Figure 2: Scenarios for the order of the thermal QCD transition as a function of N_f degenerate flavours [10].

2. The Columbia plot for mass-degenerate quarks and tricritical scaling

The analysis of the chiral phase transition is facilitated by considering only mass-degenerate quarks with the partition function (in continuum notation)

$$Z(N_{\mathrm{f}}, g, m) = \int \mathcal{D}A_\mu \left(\det M[A_\mu, m] \right)^{N_{\mathrm{f}}} e^{-\mathcal{S}_{\mathrm{YM}}[A_\mu]} . \tag{1}$$

This can formally be viewed as a statistical system depending on a continuous parameter N_{f}, which allows for an alternative interpolation between $N_{\mathrm{f}} = 2$ and $N_{\mathrm{f}} = 3$, rather than varying the strange quark mass. The Columbia plots of figure 1 then translate to the analogous versions of figure 2. Looking at the problem from this perspective offers two important benefits: First, since there is no chiral phase transition for $N_{\mathrm{f}} = 1$, a first-order transition in the chiral limit for any $N_{\mathrm{f}} > 1$ must necessarily weaken with decreasing N_{f}, until it vanishes in a tricritical point. This is because a first-order transition in the chiral limit represents a coexistence of three states, with $\pm\langle\bar\psi\psi\rangle \neq 0$ and $\langle\bar\psi\psi\rangle = 0$, and the point where the diminishing latent heat vanishes is tricritical. Hence, both the second-order *and* the first-order scenario for $N_{\mathrm{f}} = 2$ now feature a tricritical point in the Columbia plot, with either $2 < N_{\mathrm{f}}^{\mathrm{tric}} < 3$ or $1 < N_{\mathrm{f}}^{\mathrm{tric}} < 2$, respectively. Second, the Z_2-critical line, which separates the parameter region with analytic crossover from that of first-order transitions, enters the tricritical point as a function of the symmetry breaking scaling field $(am)^{2/5}$,

$$N_{\mathrm{f}}^c(am) = N_{\mathrm{f}}^{\mathrm{tric}} + \mathcal{A}_1 \, (am)^{2/5} + \mathcal{A}_2 \, (am)^{4/5} + \dots . \tag{2}$$

The critical exponents of the scaling field take known mean field values, since the upper critical dimension for a tricritical point is three [15]. On the lattice, there will be an additional dependence on N_τ, viz. the lattice spacing, and hence a tricritical line. Based on these facts, and with explicit first-order transitions seen on coarse lattices, our task is now reduced to locating the chiral intercept $N_{\mathrm{f}}^{\mathrm{tric}}(N_\tau)$ based on a polynomial with known exponents, rather than having to distinguish between different sets of critical exponents.

3. Simulations and analysis

For our numerical investigation, we use the standard unimproved Wilson gauge and staggered fermion actions. All numerical simulations have been performed using the publicly available OpenCL-based code CL²QCD, which is optimised to run efficiently on AMD GPUs and contains an implementation of the RHMC algorithm for unimproved rooted staggered fermions. Version v1.0 [16] has been employed for simulations on smaller N_τ on the L-CSC supercomputer at GSI, while version v1.1 [17] has been run on the HLR supercomputer at Goethe University to run the most costly simulations. The thousands of necessary simulations were efficiently handled by the BaHaMAS software [18].

Our method to determine the order of the chiral transition by finite size scaling is standard. We evaluate the chiral condensate $\langle \bar{\psi}\psi \rangle$, which becomes an exact order parameter in the massless limit, and its standardised cumulants $B_{3,4}$ defined as

$$B_n(\beta, am, N_{\rm f}, N_\tau, N_\sigma) = \frac{\left\langle \left(\bar{\psi}\psi - \langle \bar{\psi}\psi \rangle \right)^n \right\rangle}{\left\langle \left(\bar{\psi}\psi - \langle \bar{\psi}\psi \rangle \right)^2 \right\rangle^{n/2}} \ . \tag{3}$$

For any fixed volume, the bare parameter space of unimproved staggered fermions is four-dimensional, $(\beta, am, N_{\rm f}, N_\tau)$. We first locate the phase boundary between chirally broken and restored regions by the condition of vanishing skewness for the distribution of the chiral condensate, typically by scanning in β, $B_3(\beta_c, am, N_{\rm f}, N_\tau, N_\sigma) = 0$. This defines a three-dimensional subspace, which is composed of a region of crossover transtions and a region of first-order transitions. These are separated by a Z_2-critical surface, to be identified by the parameter values where the kurtosis assumes its 3D Ising value, $B_4(\beta_c, am_c, N_{\rm f}, N_\tau, N_\sigma = \infty) = 1.604$. On finite but sufficiently large volumes close to the thermodynamic limit, the kurtosis can be expanded about the critical point,

$$B_4(\beta_c, am, N_{\rm f}, N_\tau, N_\sigma) = 1.604 + \mathcal{B}_1(\beta_c, N_{\rm f}, N_\tau)\,(am - am_c)N_\sigma^{1/\nu} + \dots , \tag{4}$$

through which it passes smoothly. As the volume is increased, this approaches a step function and the rate of the approach to the thermodynamic limit is governed by a 3D Ising critical exponent, $\nu = 0.6301$. Dots in the equation indicate additional terms that vanish in the infinite volume limit. For the set of aspect ratios $N_\sigma/N_\tau \in \{2, 3, 4, 5\}$ used throughout, the corrections were found to be statistically insignificant in most cases, so that fits to this equation provide estimates for the critical masses, and hence the location of the Z_2-critical surface in infinite volume.

For each parameter combination, we generally simulated four independent Monte Carlo chains until their B_4-values agreed to within three standard deviations or better, upon which they were merged. In order to tune precisely to the phase boundary, the multi-histogram method was used to interpolate between simulated β-values [19]. All steps of our analysis follow the details described in [10, 20]. In addition to those, we have implemented a new error analysis for the critical masses am_c based on bootstrap estimators, which is entirely independent of the usual χ^2-minimisation. Besides providing a crucial reliability check on the fits, this procedure typically produces slightly smaller errors [21]. Altogether, the following results are based on 120 million Monte Carlo trajectories spread over 600 different parameter combinations, obtained over a span of several years.
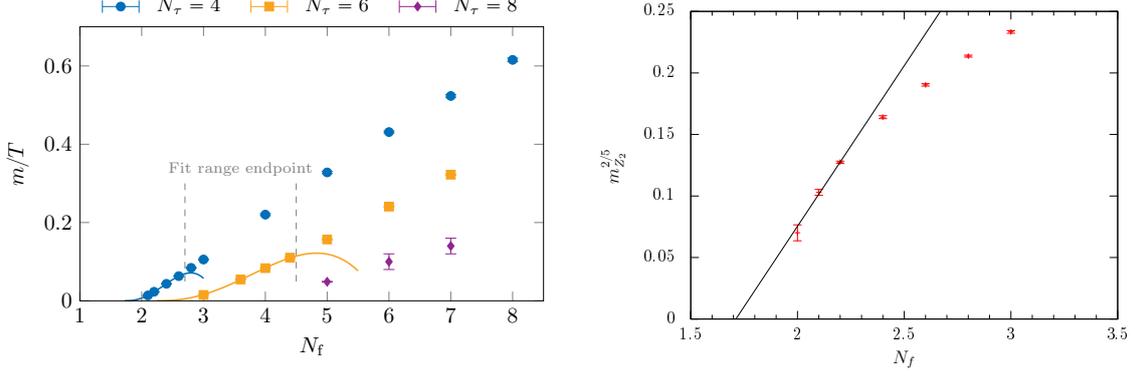
(a) Critical mass in units of T. Lines represent next-to-leading order scaling fits to equation (5) [21].

(b) Critical mass in lattice units, with a leading-order scaling fit to equation (5). From [10].

Figure 3: The chiral critical surface projected onto the (am, N_f)-plane. Regions above the lines represent crossover transitions, those below first-order transitions.

4. The bare parameter space of staggered lattice QCD

The result of our finite size scaling analysis is the location of the chiral critical surface in the infinite volume bare parameter space of the lattice theory. To analyse its implications, we study its projections onto all possible planes of variable pairings. We start with figure 3(a), which represents the lattice analogue for the sketched Columbia plots in figure 2. The data represent the chiral critical surface corresponding to different fixed N_τ, separating crossover transitions above from first-order transitions below. One clearly observes a strenghtening of the first-order transition with increasing N_f and a weakening with increasing N_τ. Moreover, there is no sign of convergence towards a continuum limit yet. Thus, large parts of the first-order region must be a cutoff effect, which is evidently stronger for larger N_f. Our main interest is in the intercept of the curves with the lattice chiral limit, i.e. the tricritical line $N_f^{\text{tric}}(N_\tau)$. Tricritical scaling can be appreciated in the rescaled figure 3(b), where earlier $N_\tau = 4$ data approach a leading order scaling relation [10]. This allows for an extrapolation

$$am_c\big(N_f(N_\tau), N_\tau\big) = \mathcal{D}_1(N_\tau)\big(N_f - N_f^{\text{tric}}(N_\tau)\big)^{5/2} + \mathcal{D}_2(N_\tau)\big(N_f - N_f^{\text{tric}}(N_\tau)\big)^{7/2} + \dots, \qquad (5)$$

where we inverted equation (2), since the N_f-values are exact while am_c has errors. Note also that the $N_f = 2$ data point in figure 3(b) has been obtained by a tricritical extrapolation in imaginary chemical potential at fixed $N_f = 2$ [8]. This is an independent confirmation of the bare quark mass as a tricritical scaling field near its chiral limit. Unfortunately, the scaling region is small in this variable pairing. Next-to-leading order fits in the left figure predict $N_f^{\text{tric}}(N_\tau = 4) \approx 1.71(3)$ and $N_f^{\text{tric}}(N_\tau = 6) \approx 2.20(8)$. One concludes that, for unimproved staggered fermions, the $N_f = 2$ massless theory shows a first-order transition on $N_\tau = 4$, but a second-order transition on all finer lattices and in the continuum. The question is what happens to the $N_f \geq 3$ theories, since the $N_\tau = 8$ data suggest a further slide of the critical line towards larger N_f.
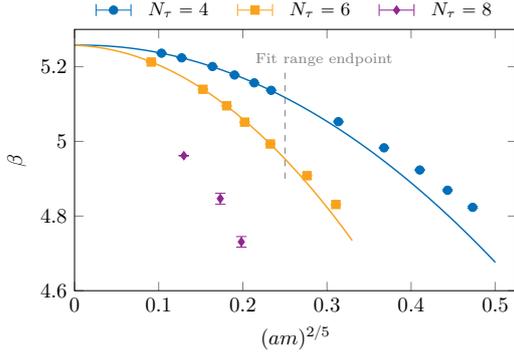
Figure 4: Chiral critical surface projected onto the (β, am)-plane, fitted to next-to-leading order tricritical scaling. From [21].
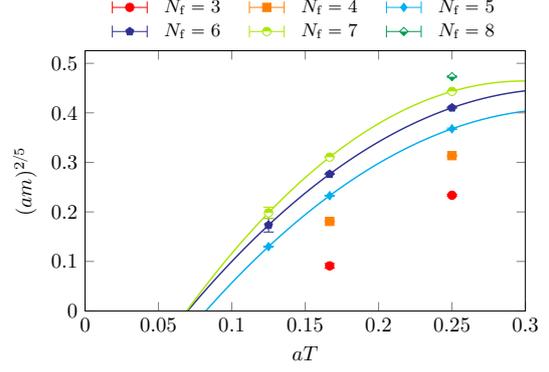

Figure 5: Chiral critical surface projected onto the $(am, aT = N_\tau^{-1}))$-plane, interpolated by next-to-leading order tricritical scaling. From [21].

More information can be obtained by analysing the same data in different variable pairings. First, figure 4 clearly confirms the tricritical scaling behaviour, which does not get superseded by the linear $N_{\rm f}$-dependence observed in figure 3(a). The critical lines are implicitly parametrised by $N_{\rm f}$, the region above them corresponds to crossover transitions, and those below to first-order transitions. The lower β-axis represents a first-order triple line that ends in the tricritical point marked by the intercept of the curves with the lattice chiral limit.

In figure 5 we show the rescaled critical bare quark masses plotted as a function of N_τ. Only a slight curvature is exhibited by those $N_{\rm f}$ with three data points, which thus are compatible with next-to-leading order scaling and a tricritical point at some finite $N_\tau^{\rm tric}(N_{\rm f})$. Note however, that for fixed $N_{\rm f}$-values a tricritical point is not guaranteed to exist, and one must test for the functional behaviour. As an example, figure 6 shows fits to the $N_{\rm f} = 5$ data assuming different scenarios. For a first-order chiral transition there is a finite continuum critical mass m_c, modified by the usual polynomial discretisation effects, so that in lattice units one has

$$am_c(N_\tau, N_{\rm f}) = \tilde{\mathcal{F}}_1(N_{\rm f})\, aT + \tilde{\mathcal{F}}_2(N_{\rm f})\, (aT)^2 + \tilde{\mathcal{F}}_3(N_{\rm f})\, (aT)^3 + \dots . \tag{6}$$

Two different next-to-leading order fits shown in figure 6(a) have $\chi^2_{\rm dof} > 50$ and visibly fail to describe the data. By contrast, a description with a tricritical point is possible, interpolating with the scaling form, which needs to be inverted again,

$$aT_c(am, N_{\rm f}) = aT_{\rm tric}(N_{\rm f}) + \mathcal{E}_1(N_{\rm f})(am)^{2/5} + \mathcal{E}_2(N_{\rm f})(am)^{4/5} + \dots , \tag{7}$$

$$\left(am_c(N_\tau, N_{\rm f})\right)^{2/5} = \mathcal{F}_1(N_{\rm f})\big(aT - aT_{\rm tric}(N_{\rm f})\big) + \mathcal{F}_2(N_{\rm f})\big(aT - aT_{\rm tric}(N_{\rm f})\big)^2 + \dots . \tag{8}$$

This gives the central line in figure 6(b). Fits corresponding to the inverted equation (7) with $\mathcal{E}_1 = 0$ or $\mathcal{E}_2 = 0$ bound this intercept and give a measure of uncertainty. Our current data for $N_{\rm f} = 5$ are thus consistent with a tricritical point at $N_\tau^{\rm tric}(N_{\rm f} = 5) \approx 12.5$, and the same holds for $N_{\rm f} = 6, 7$ with slightly larger $N_\tau^{\rm tric}$, cf. figure 5. This observation is fully compatible with the one made in figure 3(a): in the lattice chiral limit $am = 0$ there is a monotonically rising tricritical line $N_{\rm f}^{\rm tric}(N_\tau)$.

This has profound consequences for the approach to the continuum chiral limit. Avoiding lattice artefacts requires to take the continuum limit before the chiral limit. Since the continuum
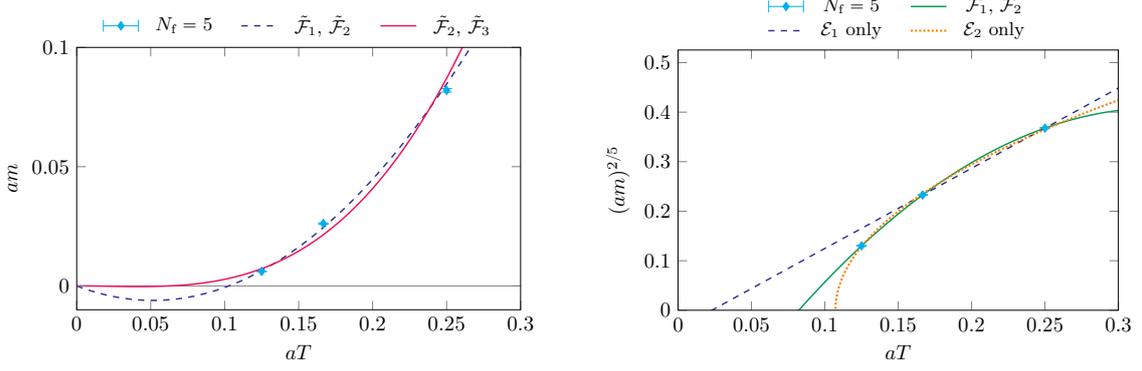
(a) Fits to equation (6), corresponding to the first-order scenario. From [21].

(b) Fits to equations (7) and (8), corresponding to the second-order scenario. From [21].

Figure 6: Fitting and extrapolating the chiral critical line of the $N_{\mathrm{f}} = 5$ theory.

limit is represented by the origin in figure 5, the existence of a tricritical point $N_{\tau}^{\mathrm{tric}}(N_{\mathrm{f}})$ implies that the continuum chiral limit is inevitably approached from the crossover region, and hence can only represent a second-order transition. In figure 5 this appears to be the case for all $N_{\mathrm{f}} \in [2, 7]$, which would then all feature second-order transitions in their respective continuum chiral limits.

5. Wilson fermions

In view of our surprising findings from the last sections, it is particularly important to do a similar analysis in a different discretisation scheme. To this end, we re-analyse already published data [7, 11, 12] for the critical pseudo-scalar mass delimiting the first-order transition for $N_{\mathrm{f}} = 3$ $O(a)$-improved Wilson fermions with $N_{\tau} \in [4, 12]$. This is shown in figure 7, where we have employed $am_{PS}^2 \propto am$ in order for the vertical axis to represent the scaling field, i.e. the (additively renormalised) quark mass.

The lines in the figure represent leading-order scaling fits to $N_{\tau} \in [8, 12]$ and next-to-leading order scaling fits to $N_{\tau} \in [6, 12]$ as well as to $N_{\tau} \in [4, 8]$. An excellent description of the data is achieved in all three cases with χ_{dof}^2 near 1 and only small variation of the intercept, which represents a $N_{\tau}^{\mathrm{tric}}(N_{\mathrm{f}} = 3)$ for this non-perturbatively improved Wilson discretisation. This confirms the viability of our staggered analysis based on $N_{\tau} \in [4, 8]$, and it leads to the same conclusion: the first-order chiral phase transitions observed for $N_{\mathrm{f}} = 3$ $O(a)$-improved Wilson fermions are not connected to the the continuum chiral limit, which therefore must represent a second-order transition.

6. Conclusions

In summary, we have exploited the fact that a change of the massless chiral phase transition from first to second order as a function of either N_{f} or lattice spacing must pass through a tricritical point. Its location can be determined by tricritical scaling of the Z_2-critical line, which separates the first-order phase transitions from crossover behaviour and extrapolates to a tricritical point in
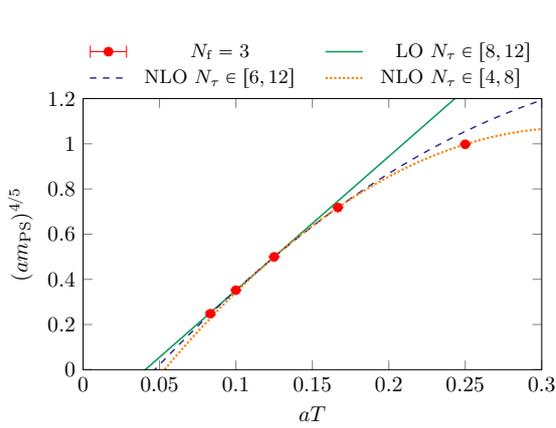
Figure 7: Chiral critical line for $N_f = 3$ $O(a)$-improved Wilson fermions, with various fits to tricritical scaling. The data are taken from [12], the figure from [21].
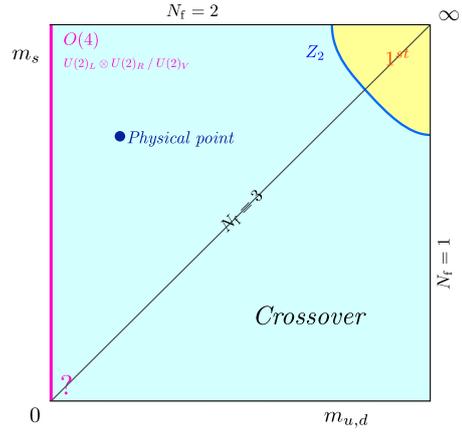

Figure 8: Continuum Columbia plot suggested by our results. The chiral transition is of second order for all values of m_s, its universality class is not determined here. From [21].

the chiral limit. A comprehensive analysis of this boundary for unimproved staggered quarks on lattices with $N_\tau \in \{4, 6, 8\}$ is consistent with all $N_f \in [2, 7]$ displaying such a tricritical point. This implies that the first-order region is not connected to the continuum limit which, therefore, must correspond to a second-order transition. The same result is found for $N_f = 3$ $O(a)$-improved Wilson fermions. These conclusions can only be avoided if future results for the chiral critical line on larger N_τ break off the tricritical scaling curves. However, based on the currently available data one would have to conclude that the Columbia plot looks as in figure 8. All results reported here have been published in [21]. Finally, we note that our analysis can be applied to any discretisation with explicit first-order transitions. This should allow to fully settle the question of the order of the massless chiral phase transition in the near future.

Acknowledgments

References

[1] F.R. Brown, F.P. Butler, H. Chen, N.H. Christ, Z.-H. Dong, W. Schaffer et al., *On the existence of a phase transition for QCD with three light quarks*, *Phys. Rev. Lett.* **65** (1990) 2491.

[2] R.D. Pisarski and F. Wilczek, *Remarks on the Chiral Phase Transition in Chromodynamics*, *Phys. Rev.* **D29** (1984) 338.

[3] Y. Iwasaki, K. Kanaya, S. Kaya, S. Sakai and T. Yoshie, *Finite temperature transitions in lattice QCD with Wilson quarks: Chiral transitions and the influence of the strange quark*, *Phys. Rev. D* **54** (1996) 7010 [`hep-lat/9605030`].

[4] F. Karsch, E. Laermann and C. Schmidt, *The Chiral critical point in three-flavor QCD*, *Phys. Lett.* **B520** (2001) 41 [`hep-lat/0107020`].

[5] P. de Forcrand and O. Philipsen, *The QCD phase diagram for three degenerate flavors and small baryon density*, *Nucl. Phys.* **B673** (2003) 170 [`hep-lat/0307020`].

[6] P. de Forcrand, S. Kim and O. Philipsen, *A QCD chiral critical point at small chemical potential: Is it there or not?*, *PoS* **LAT2007** (2007) 178 [`0711.0262`].

[7] X.-Y. Jin, Y. Kuramashi, Y. Nakamura, S. Takeda and A. Ukawa, *Critical endpoint of the finite temperature phase transition for three flavor QCD*, *Phys. Rev. D* **91** (2015) 014508 [`1411.7461`].

[8] C. Bonati, P. de Forcrand, M. D'Elia, O. Philipsen and F. Sanfilippo, *Chiral phase transition in two-flavor QCD from an imaginary chemical potential*, *Phys. Rev.* **D90** (2014) 074030 [`1408.5086`].

[9] O. Philipsen and C. Pinke, *The $N_f = 2$ QCD chiral phase transition with Wilson fermions at zero and imaginary chemical potential*, *Phys. Rev.* **D93** (2016) 114507 [`1602.06129`].

[10] F. Cuteri, O. Philipsen and A. Sciarra, *QCD chiral phase transition from noninteger numbers of flavors*, *Phys. Rev. D* **97** (2018) 114511 [`1711.05658`].

[11] X.-Y. Jin, Y. Kuramashi, Y. Nakamura, S. Takeda and A. Ukawa, *Critical point phase transition for finite temperature 3-flavor QCD with non-perturbatively O(a) improved Wilson fermions at $N_t = 10$*, *Phys. Rev.* **D96** (2017) 034523 [`1706.01178`].

[12] Y. Kuramashi, Y. Nakamura, H. Ohno and S. Takeda, *Nature of the phase transition for finite temperature $N_f = 3$ QCD with nonperturbatively O(a) improved Wilson fermions at $N_t = 12$*, *Phys. Rev. D* **101** (2020) 054509 [`2001.04398`].

[13] A. Bazavov, H.T. Ding, P. Hegde, F. Karsch, E. Laermann, S. Mukherjee et al., *Chiral phase structure of three flavor QCD at vanishing baryon number density*, *Phys. Rev. D* **95** (2017) 074505 [`1701.03548`].

[14] O. Philipsen, *Lattice Constraints on the QCD Chiral Phase Transition at Finite Temperature and Baryon Density*, *Symmetry* **13** (2021) 2079 [`2111.03590`].

[15] I. Lawrie and S. Sarbach, *Theory of tricritical points*, in *Phase transitions and critical phenomena*, C. Domb and J. Lebowitz, eds., vol. 9, p. 1 (1984).

[16] C. Pinke, M. Bach, A. Sciarra, F. Cuteri, L. Zeidlewicz, C. Schäfer et al., `CL`^{2}`QCD -- v1.0`, Sept., 2018. 10.5281/zenodo.5121895.

[17] A. Sciarra, C. Pinke, M. Bach, F. Cuteri, L. Zeidlewicz, C. Schäfer et al., *CL^{2}QCD -- v1.1*, Feb., 2021. 10.5281/zenodo.5121917.

[18] A. Sciarra, *BaHaMAS*, Feb., 2021. 10.5281/zenodo.4577425.

[19] A.M. Ferrenberg and R.H. Swendsen, *Optimized monte carlo data analysis*, *Phys. Rev. Lett.* **63** (1989) 1195.

[20] F. Cuteri, O. Philipsen, A. Schön and A. Sciarra, *Deconfinement critical point of lattice QCD with N_f=2 Wilson fermions*, *Phys. Rev. D* **103** (2021) 014513 [2009.14033].

[21] F. Cuteri, O. Philipsen and A. Sciarra, *On the order of the QCD chiral phase transition for different numbers of quark flavours*, *JHEP* **11** (2021) 141 [2107.12739].

PoS(LATTICE2021)458